

# Modelling an Energy Efficient UPS Based on Modular Multilevel Design

Ekaterina Trusova<sup>1,\*</sup> Victor Lavrinovskiy<sup>1</sup> Anastasia Fedorkova<sup>1</sup>  
Vladimir Simukhin<sup>1</sup> Aleksei Romanenko<sup>2</sup>

<sup>1</sup> Saint Petersburg Electrotechnical University "LETI", St. Petersburg, Russia

<sup>2</sup> LUT University, Lappeenranta, Finland

\*Corresponding author. Email: [estrusova@stud.etu.ru](mailto:estrusova@stud.etu.ru)

## ABSTRACT

This article discusses the utilization of a modular multi-level structure for the construction of an energy-efficient uninterruptible power supply. The benefits and disadvantages of the modular structure are considered. The relevance of this topic is that such a structure makes it possible to significantly simplify the conversion of electrical energy. Modular multi-level converters do not require additional transformers or filters, which significantly reduces losses and increases energy efficiency. It is also enough to simply replace failed element with a similar one.

**Keywords:** Modular multilevel converter, Uninterruptible power supply, Energy storage, Energy efficiency, Bridge cell.

## 1. INTRODUCTION

Nowadays, there is a tendency to use more energy-efficient power converters. Earlier to build a block with semiconductor elements fully controlled keys and thyristors were needed, now the transition to controlled keys and transistors is underway. This solution allows for two-way energy exchange, power factor regulation and an acceptable harmonic composition of the current consumed from the network.

Classical schemes of power active rectifiers of powerful electric drives usually represent a connection of several three-level converters connected to the network through a step-down transformer. Multi-pulse connection schemes of transformer windings are also used to reduce the distortion of the sinusoidal curve of the network current. Such configurations represent a serial connection of the primary windings of the transformer and various groups of connections of the secondary windings.

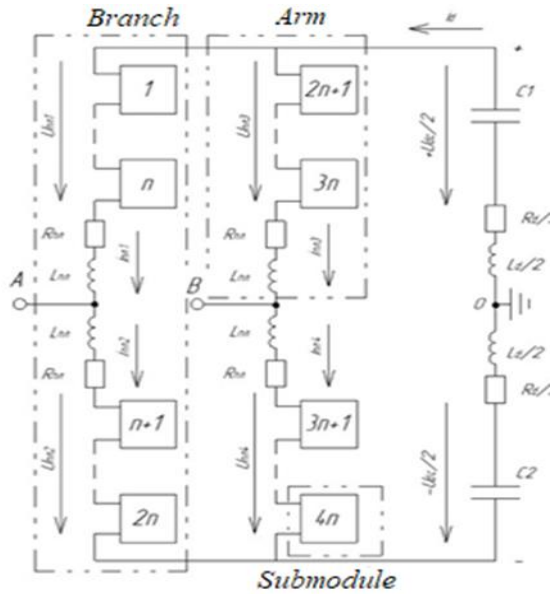
In modern conditions of gradual reduction in the cost of transistors and rising prices for active materials of transformers, a fundamentally new direction of development of frequency converters is being formed, which consists in designing energy-efficient "transformer-free" multi-level converters based on modular designs [1].

The concept of MMC was first proposed in 2001 and 2003 in the works of Marquardt and Lesnicar [2]–[3].

The article will consider an energy-efficient transformer-free UPS based on a modular multilevel structure.

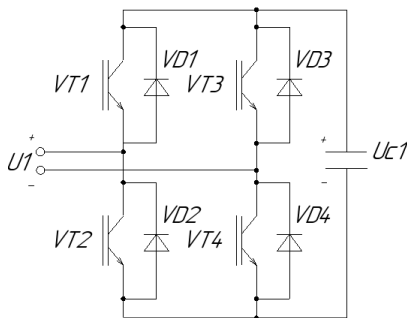
## 2. CONVERTER CIRCUIT DESCRIPTION

Figure 1 shows a block diagram of a modular multilevel converter. The converter includes two phase branches A, B, each of which contains two arms. Each arm consists of  $n$  identical submodules (cells) connected in series and a current-limiting inductance  $L_{pl}$ , as well as an active resistance  $R_{pl}$ , taking into account switching losses in semiconductors [1].



**Figure 1** Block diagram of a modular multilevel converter.

Bridge cells are used to build multi-level converters, an example of which is shown in Figure 2.



**Figure 2** Schematic of a typical bridge cell.

These converters also have such feature as a high degree of modularity. Each submodule can be considered as a submodule with a similar circuit topology, control and modulation structure.

Therefore, in case of a malfunction in one of these cells, it is possible to replace it quickly and easily. Moreover, using the appropriate control method, it is possible to bypass the faulty pod module without disconnecting the load, which entails long-term operability [4].

### 3. MATHEMATICAL DESCRIPTION OF UPS BASED ON MMS

It is necessary to determine the fraction of time during which the switches are in a conducting state before modelling a converter. This control method cannot be fully applied for MMC, since during the operation of the converter, some of the submodules are switched on, while others are shunted. The inclusion of a submodule in one arm of the branch is accompanied

by synchronous disconnection of the submodule in the other arm [5].

The choice of storage voltage is based on the operating voltage of the converter and the number of submodules. Due to the small change in battery voltage during discharge, it is possible to maintain a voltage of  $\pm 10\%$  of the nominal without complex balancing algorithms.

The mathematical model of the circuit presented below is developed with several assumptions: the switching frequency is considered infinite and the number of submodules is also infinite. Figure 3 is provided to illustrate the calculations.

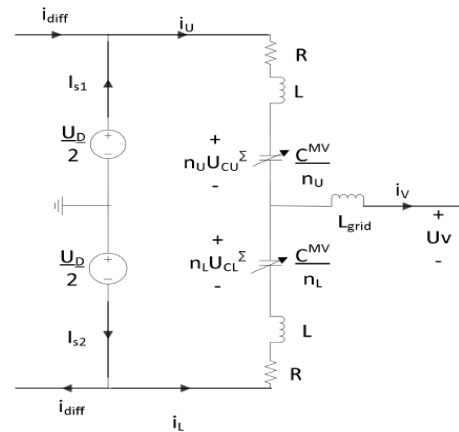


**Figure 3** Equivalent scheme of MMC operation.

Table 1 shows the symbols used in the description of the mathematical model.

**Table 1.** The parameters

$U_d$	DC pole to pole voltage
$U_v$	Output AC voltage
$U_{cu}^\Sigma$	Sum of capacitor voltages in upper arm
$U_{cl}^\Sigma$	Sum of capacitor voltages in lower arm
$e_v$	Inner alternating voltage
$i_U$	Current in the upper arm
$i_L$	Current in the lower arm e
$i = i_U + i_L$	Output AC current
$i_{diff}$	Circulating current
$n_U$	Insertion index in upper arm
$n_L$	Insertion index in lower arm

The currents of cells are obtained by using the Kirchoff's law:

$$i_U + i_L = i_v \quad (1)$$

$$i_U = I_{s1} + i_{diff} \quad (2)$$

$$i_L = I_{s2} - i_{diff} \quad (3)$$

Substituting Equation (2) and Equation (3) into Equation (1), the following expression (4) can be obtained:

$$i_V = I_{s1} + i_{diff} + I_{s2} - i_{diff} = I_{s1} + I_{s2} \quad (4)$$

The difference between the cell currents will be:

$$\begin{aligned} i_U - i_L &= I_{s1} + i_{diff} - (I_{s2} - i_{diff}) = \\ &= I_{s1} - I_{s2} + 2I_{diff} \end{aligned} \quad (5)$$

In each phase of the converter there are 2N submodules with N submodules in each arm. At each moment of time in the entire phase N modules have on state and N modules are shunted. The insertion index of each submodule is entered  $n_m = \frac{1}{N}$  if the module is enabled and  $n_m = 0$  if the module is shunted. Then the sum of the voltages of all working capacitors will be defined by Equation (6):

$$U_{Cm} = n_m U_{Cm}^\Sigma \quad (6)$$

where  $U_{Cm}^\Sigma$  – the total voltage of the capacitors in the arm.

The insertion index of the phase submodules of the converter should remain equal to one, since switching cells of one arm corresponds to disconnecting submodules in the other arm. Mathematically, it is described as Equation (7):

$$n_U + n_L = 1 \quad (7)$$

Voltages can be obtained Kirchoff's law (Equations (8–9)):

$$\frac{U_D}{2} - n_U U_{CU}^\Sigma - U_V - \left( R i_{diff} + L \frac{di_{diff}}{dt} \right) - L_{grid} \frac{di_V}{dt} = \quad (8)$$

$$= R I_{s1} + L \frac{dI_{s1}}{dt}$$

$$-\frac{U_D}{2} + n_L U_{CL}^\Sigma - U_V + \left( R i_{diff} + L \frac{di_{diff}}{dt} \right) - L_{grid} \frac{di_V}{dt} = \quad (9)$$

$$= R I_{s2} + L \frac{dI_{s2}}{dt}$$

Assuming that:

$$I_{s1} = I_{s2} \quad (10)$$

Then the following Equation (11) can be obtained from Equations (9–10):

$$U_D - n_U U_{CU}^\Sigma - n_L U_{CL}^\Sigma = 2 \left( R i_{diff} + L \frac{di_{diff}}{dt} \right) \quad (11)$$

With an ideal voltage balancing of the converter arms  $U_{CU}^\Sigma = U_{CL}^\Sigma = U_D$ , the deviation  $U_D$  will be zero. Circulating currents are the result of not perfectly balanced voltages of several cells. If the deviation  $U_D$  is zero, therefore, the steady-state value  $i_{diff}$  will also be zero.

Using Equation (10) in Equation (4) the Equation (12) can be obtained:

$$I_{s1} = I_{s2} = \frac{i_V}{2} \quad (12)$$

Equation (13) can be obtained from Equation (5):

$$i_{diff} = \frac{I_U - I_L}{2} \quad (13)$$

After converting Equations (9–10), the following Equation (14) can be obtained:

$$\begin{aligned} R(i_U + i_L) + L \frac{d(i_U + i_L)}{dt} + 2L_{grid} \frac{di_V}{dt} + 2U_V = \\ = n_L U_{CL}^\Sigma - n_U U_{CU}^\Sigma \end{aligned} \quad (14)$$

The following substitution (Equation (15)) can be performed in the Equation (14):

$$L^* = \frac{L}{2} + L_{grid} \quad (15)$$

Equation (16) can be obtained by converting Equation (1):

$$U_V = \frac{1}{2} (n_L U_{CL}^\Sigma - n_U U_{CU}^\Sigma) - \frac{R}{2} i_V - L^* \frac{di_V}{dt} \quad (16)$$

This dependence (Equation (16)) describes that the output voltage  $U_V$  depends on the output current  $i_V$ , as well as on the arm voltages of the converter  $n_U U_{CU}^\Sigma$  and  $n_L U_{CL}^\Sigma$ . The difference between these voltages can be considered as an internal voltage equal to Equations (17–18):

$$e_V = \frac{1}{2} (n_L U_{CL}^\Sigma - n_U U_{CU}^\Sigma) \quad (17)$$

$$U_V = e_V - \frac{R}{2} i_V - L^* \frac{di_V}{dt} \quad (18)$$

Equation (16) can also be rewritten in the dq coordinate system by using the Laplace transform. The result of such a conversion is described by the Equations (19–20):

$$V_d = e_{vd} - \left( \frac{R}{2} + sL^* \right) i_d - \omega L^* i_q \quad (19)$$

$$V_q = e_{vq} - \left( \frac{R}{2} + sL^* \right) i_q - \omega L^* i_d \quad (20)$$

It is customary to make a control loop of the active component along the d axis, while developing of control algorithms. Since Equations (19–20) are symmetric, it is customary to reduce control along the q axis to zero and then control is carried out in accordance with Equation (19).

### 3.1. Algorithm for regulating arm tension

The purpose of this algorithm is to select the best configuration of the arm cells to maintain the necessary voltage between the arm capacitors. Depending on the direction of the current flowing through the cell, the voltage of the capacitor changes or remains unchanged. Some structural cells will require more energy than others without proper regulation of these voltages that can lead to charging some and discharging others. Thus, in order to maintain the voltage in the arm, it is necessary to ensure that the power entering and outgoing from the submodules are the same [6]. The algorithm for regulating the shoulder tension is shown in Figure 4.

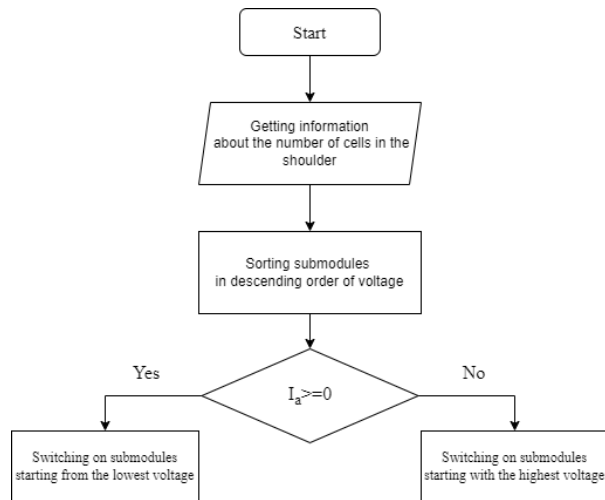


Figure 4 Algorithm for regulating arm tension.

In each cycle of the algorithm, the voltage of submodules in one arm is measured. Then they are sorted in descending order of magnitude and the number of cells to be included in the work is determined. If the shoulder current has a positive direction or is zero, then the submodules with the lowest voltage value will be connected first, otherwise the modules with the highest voltage will be put into operation.

### 3.2. Control of circulating currents

The inequality of internal voltages between the branches generates so-called circulating currents. They have the form of an inverse sequence with twice the frequency of the carrier harmonic. These currents increase the RMS values of the converter arm currents, which leads to increased losses in the converter such as loss of conductivity of keys and losses in capacitors.

According to [7], the internal unbalanced voltage can be determined as Equation (21):

$$u_{diff} = L \frac{di_{diff}}{dt} + Ri_{diff} \quad (21)$$

Figure 5 shows the loops of the upper and lower arms.

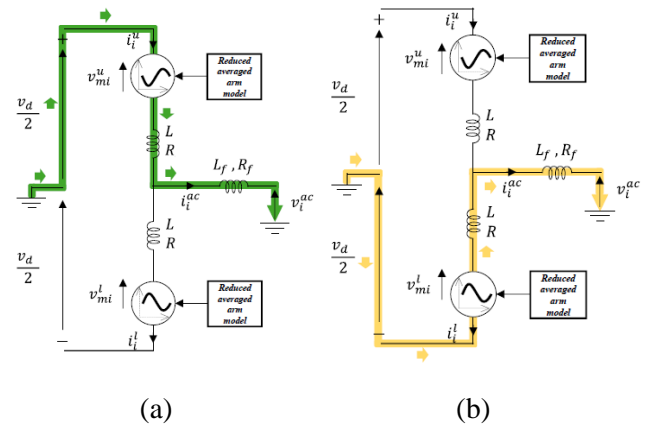


Figure 5 Operating circuits of the upper (a) and lower (b) arms.

Based on the Equation (21), it can be mentioned that the circulating current depends on a given voltage, therefore, it can be controlled by changing the value of the unbalanced voltage. The following Equations (22–23) can be obtained from Equations (17–21):

$$n_U U_{CU}^\Sigma = \frac{U_D}{2} - e_v - u_{diff} \quad (22)$$

$$n_L U_{CL}^\Sigma = \frac{U_D}{2} + e_v - u_{diff} \quad (23)$$

The internal voltage  $e_v$  is used to regulate the loop of the external system as described above. Equations (22–23) describe that the unbalanced voltage is used to control the internal dynamic characteristics of the MMC, including circulating currents.

### 3.3. Load current regulation

Figure 6 shows a block diagram of the control of the active load current along the d axis.

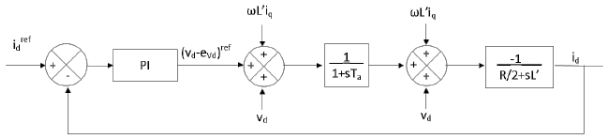


**Figure 6** Block diagram to control the active load current.

This circuit consists of a PI controller, a block representing a converter that implements a time delay, and an electrical circuit block described by Equation (19). Because of symmetry of Equations (19–20), it can be assumed that the control loop along the q axis will be similar to the contour shown in Figure 6, so the control in the q axes is usually reduced to zero. An error signal is received at the input of the PI controller in other words error signal is the difference between the reference signal and the feedback signal.

The transfer function of the converter can be written as Equation (24):

$$H_{conv}(s) = \frac{1}{1 + T_a s} \quad (24)$$

where  $T_a$  – delay time.

The transfer function of the PI controller is described by Equation (25):

$$H_{Cc}(s) = K_{pc} \frac{1 + T_{ic} s}{T_{ic} s} \quad (25)$$

where  $K_{pc}$  – proportionality coefficient;  $T_{ic}$  – time constant.

Transfer function of a block imitating an electrical circuit is described by Equation (26):

$$H_{el}(s) = \frac{1}{R' + sL'} = \frac{1}{1 + s\tau_{el}} \quad (26)$$

where  $\tau_{el} = \frac{L'}{R'}$  – the time constant of the transient process.

The transfer function of the open loop of current control can be obtained by multiplying the dependencies (24), (25) and (26) and it is described by the Equation (27):

$$H_{c,OL} = K_{pc} \frac{1 + T_{ic} s}{T_{ic} s} \frac{1}{1 + T_a s} \frac{-1}{\frac{R}{2} + L' s} \quad (27)$$

#### 4. MODEL DESCRIPTION

Figure 7 shows the power part of the model of a transformer-free single-phase rectifier being developed based on a modular multilevel structure.

The power part of this model consists of four “Subsystem” blocks, which are the arms of the converter. Each arm consists of three submodules represented by typical bridge cells (Figure 2). Figure 8 shows an enlarged model of the converter arm.

A PI controller is used to stabilize the output voltage.

However, the use of a PI controller requires performing a coordinate transformation, since the integral component is not able to work correctly with rapidly changing periodic signals.

Phase frequency auto-tuning is an integral part of modern converter technology and is designed to measure the phase and frequency of the voltage of an alternating signal. The methods of phase-locked frequency are divided into two large categories. The first methods are the most common and contain methods of coordinate transformations. The second methods use various kinds of oscillators and resonance effects based on them.

As a replacement for the phase-locked frequency it is possible to use a proportional resonance controller that does not require obtaining information about the network.

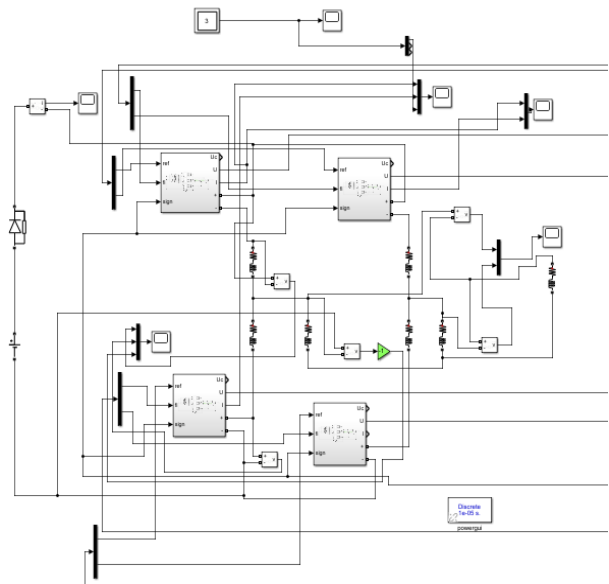


**Figure 7** Power part of the UPS.

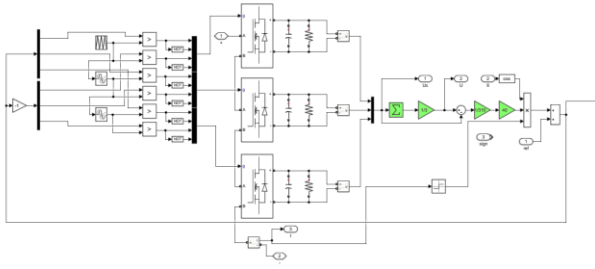


Figure 8 SIMULINK model of the converter arm.

### 5. SIMULATION RESULTS

Figures 9–11 show the results of simulating the dynamic operation modes of the model.

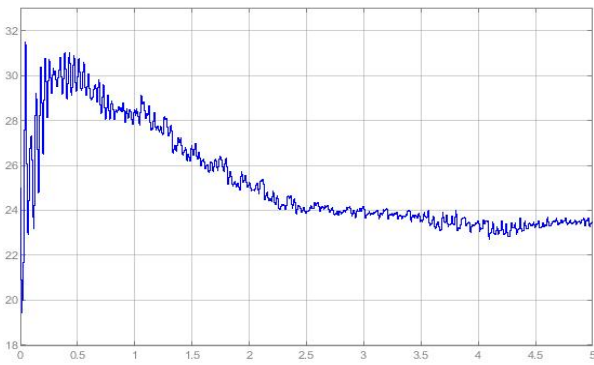


Figure 9 Instantaneous voltage values of the cell capacitor.

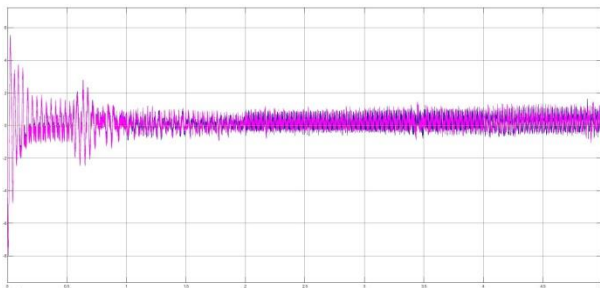


Figure 10 Circulating currents of the converter arm.

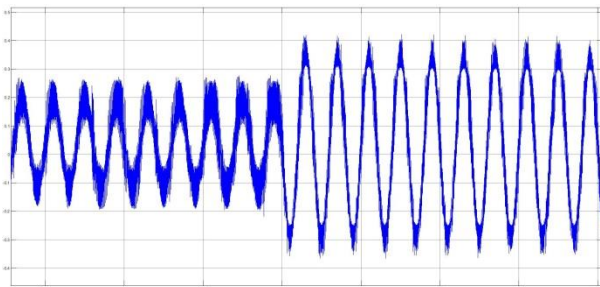


Figure 11 Instantaneous values of the converter phase current.

### 6. EVALUATION OF THE EFFICIENCY OF THE DEVELOPED UPS BASED ON MMS

The total losses for conductivity and switching are determined as Equation (28) based on [8]:

$$P_{\Sigma} = P_{cond \Sigma 1} + P_{sw} \tag{28}$$

where  $P_{cond \Sigma 1}$  – total conductivity loss of one submodule,  $P_{sw}$  – switching loss of one submodule.

The efficiency of the converter is determined by Equation (29):

$$\eta = \frac{P - nP_{\Sigma}}{P_{\Sigma}} \tag{29}$$

where  $P$  – converter power,  $n$  – number of the cells in the converter.

Comparing devices of comparable power the efficiency of a modular UPS is higher than that of a classic one. The efficiency of the modular converter is higher due to a significant reduction in switching losses in the keys, which is associated with a change in the element base as well as with the use of a multi-level structure that does not require high switching frequencies.

The efficiency of an uninterruptible power supply based on a modular multilevel structure is about 98%, which indicates its high energy efficiency.

### 7. CONCLUSION

UPS based on modular structure has some advantages:

- the capability to adapt to any levels of mains voltage by changing the number of connected cells;
- the capability of reserving cells;
- the absence of a transformer and filter.

These advantages significantly reduce the cost of equipment production and repair work and increase the energy efficiency of the converter.

UPS based on MMC allows to achieve high efficiency and, accordingly, high energy efficiency by increasing the number of semiconductor elements.

### REFERENCES

[1] Abdulvelev I.R., Khrumshin T.R., Kornilov G.P. “Analysis of the impact of voltage modulation of active rectifiers based on modular multilevel converters,” Bulletin of SUSU. Series: Energy. 2015. №3.

- [2] Marquardt R. Stromrichterschaltungen mit verteilten Energiespeichern. German Patent: DE10103031, 24 January 2001.
- [3] Lesnicar A., Marquardt R. An Innovative Modular Multilevel Converter Topology Suitable for a Wide Power Range. In Proc. Power Tech Conference, Bologna (Spain), June 2003.
- [4] Makarov V.G., Khaybrakhmanov R.N. Multilevel voltage inverters. "Overview of topologies and applications," Bulletin of the Kazan Technological University. 2016. No. 22.
- [5] Abildgaard, E.N. "Exploring the Properties of a Modular Multilevel Converter Based HVDC Link: With Focus on Voltage Capability," Power System Relations, and Control System." (2012).
- [6] Zama M. "Modeling and Control of Modular Multilevel Converters (MMCs) for HVDC applications." Electric power. Université Grenoble Alpes, 2017. English.
- [7] Q. Tu, Z. Xu and L. Xu, "Reduced Switching-Frequency Modulation and Circulating Current Suppression for Modular Multilevel Converters," in IEEE Transactions on Power Delivery, vol. 26, no. 3, pp. 2009-2017, July 2011, DOI: 10.1109/TPWRD.2011.2115258.
- [8] Jauregui D., Bo Wang, Chen R. "Power loss calculation with common source inductance consideration for synchronous buck converters", Texas Instruments. Application Report, July 2011.